A Composite Tissue Engineered Bone Material Consisting of Bone Mesenchymal Stem Cells, Bone Morphogenetic Protein 9 (BMP9) Gene Lentiviral Vector, and P3HB4HB Thermogel (BMSCs-LV-BMP9-P3HB4HB) Repairs Calvarial Skull Defects in Rats by Expression of Osteogenic Factors

Authors' Contribution:
Study Design A
Data Collection B
Statistical Analysis C
Data Interpretation D
Manuscript Preparation E
Literature Search F
Funds Collection G

BCDEF 1 Cheng Zhou
BCDF 2 Chuan Ye
BCD 1 Chen Zhao
BCF 1 Junyi Liao
BC 1 Yuwan Li
BF 1 Hong Chen
ADEG 1 Wei Huang

1 Department of Orthopedics, The First Affiliated Hospital of Chongqing Medical University, Chongqing, P.R. China
2 Department of Orthopedics, Affiliated Hospital of Guizhou Medical University, Guizhou, Guiyang, P.R. China

Corresponding Author: Wei Huang, e-mail: zhouwst88@163.com
Source of support: Departmental sources

Background: Bone tissue engineering has been proven to be an appropriate approach for treating bone defects. This study aimed to investigate the effects and mechanism of a composite tissue engineered bone material consisting of bone mesenchymal stem cells (BMSCs), bone morphogenetic protein (BMP9) gene lentiviral vector, and P3HB4HB thermogel (BMSCs-LV-BMP9-P3HB4HB) on calvarial skull defects in rats.

Material/Methods: LV-BMP9 viral vector was structured and infected to BMSCs-P3HB4HB composite scaffold, which was named as BMSCs-P3HB4HB composite bone repair material. Adipogenic differentiation was determined by oil-red O (ORO) and alkaline phosphatase (ALP) staining. Osteogenic differentiation was measured using Alizarin red staining. Cell viability was examined using Cell-Counting Kit-8 (CCK-8) assay. Protein expression of osteogenic factors, including BMP9, runt-related transcription factor 2 (RUNX2), osteocalcin (OCN), osteopontin (OPN), and osterix (OSX), was detected with Western blot assay and immunohistochemistry. mRNA of these osteogenic factors was examined by RT-PCR. Histological changes were examined with hematoxylin and eosin (H&E) and Masson's trichrome staining. Bone repair was measured using micro-computed tomography (micro-CT).

Results: BMSCs and LV-BMP9-infected BMSCs demonstrated adipogenic and osteogenic differentiation potential. BMSCs-P3HB4HB scaffold demonstrated good cell-tissue compatibility. BMSCs-LV-BMP9-P3HB4HB exhibited significantly higher osteogenic ability and cell viability of BMSCs compared to BMSCs-LV-P3HB4HB ($p<0.05$). BMSCs-LV-BMP9-P3HB4HB significantly promoted osteogenic factors (RUNX2, OCN, OPN, and OSX) expression compared to the BMSCs-LV-P3HB4HB group ($p<0.05$) in both BMSCs and in calvarial defect rats. BMSCs-LV-BMP9-P3HB4HB demonstrated stronger repair ability. BMSCs-LV-BMP9-P3HB4HB significantly alleviated pathological injury and increased collagen fiber production compared to the BMSCs-LV-P3HB4HB group ($p<0.05$).

Conclusions: BMSCs-LV-BMP9-P3HB4HB composite bone repair material can effectively repair injured skull tissues of calvarial defect rats through triggering osteogenic factors expression. The present generated bone repair material may have applications in tissue engineering in regeneration of bone defects.

MeSH Keywords: Adult Stem Cells • Endothelial Growth Factors • Osteosarcoma • Tissue Engineering

Full-text PDF: https://www.medscimonit.com/abstract/index/idArt/924666

📄 3597   ⊞ 1   📊 10   📖 35

Background

Bone defects are a common orthopedic disease that has been become a serious clinical problem, usually requiring resection of the damaged bones and repair with substitute materials [1,2]. Generally, bone defects are caused by several risk factors, including chronic infection, traumatic damage, and resection of bone tumors, and can further lead to serious clinical problems and increased morbidity [3]. The severity of bone defects is correlated with the area of bone loss and involvement of the skeletal segment. Many strategies are used for treating bone defects clinically, such as allografts, alloplastic materials, and autografts [4]. Autogenous bone grafting has become the criterion standard therapy for bone defects [5]. However, the clinical application of autogenous bone grafting is limited by the shortage of donors and by complications such as infection, pain, nerve injury, and the potential for new fractures [6].

In recent years, bone tissue engineering has become accepted as an appropriate approach for treating bone defects, which can regenerate the defected or injured bone tissues through integrating candidate cells and bone repair materials [7]. These cells-combined materials usually act as templates for guiding tissue cell growth and tissue regeneration [8]. Synthetic materials used for tissue engineering mainly include scaffolding, gels, stimuli-responsive materials, and composites, all of which demonstrate promising bone engineering potentials [9]. The bone repair materials act as matrices for bone formation, playing critical roles in bone repair. The optimal bone repair material must have a three-dimensional (3D) structure and excellent biocompatibility and biological-conductivity, must be non-cytotoxic, and must promote cell differentiation, proliferation, and adhesion [10]. The bone repair material should activate gene expression, stimulate cell proliferation, participate in physiological activity of tissues, and finally trigger the formation of bone tissues. Although many categories of tissue repair materials (such as the biomimetic composite materials) have been discovered or generated, many problems must be resolved in clinical applications, such as biocompatibility and biological-conductivity, and 2 critical issues are the appropriate balance between degradation rate of materials and growth of tissue cells and the maintenance of mechanical strength of materials.

In recent years, synthetic polymer materials have been proven to be appropriate as tissue repair materials due to their good mechanical characteristics, strength, and controllable physical characteristics [11]. However, synthetic polymer materials also have disadvantages in terms of poor biocompatibility [11]. P3HB4HB is a fourth-generation synthetic polymer material with excellent biocompatibility, superior mechanical properties, and appropriate biodegradability, and thus has been widely applied in tissue engineering [12]. Seed cells are important

for treating bone defects. BMSCs have been extensively used in tissue engineering to promote angiogenesis and osteogenesis, both of which can further facilitate new tissue growth in bone regeneration [13]. Bone mesenchymal stem cells (BMSCs) are seed cells and multi-cellular spheroids that have demonstrated improved stem-like qualities and promote differentiation ability [14]. Therefore, P3HB4HB integrating BMSCs composite material would make scaffold-based strategy promising and increasingly practicable for clinical use in bone repair.

Bone morphogenetic proteins (BMPs) are bone growth-associated factors commonly used to promote BMSCs osteogenesis and formation of new bone in animal models and *in vitro* [15]. Among BMPs, bone morphogenetic protein-9 (BMP9) has been proven to be a highly effective BMP for promoting bone formation [16]. BMP9 can also trigger the osteogenic differentiation of human umbilical cord mesenchymal stem cells by activating several signaling pathways [17]. However, it is also unknown whether BMP9 is capable of inducing osteogenic differentiation in BMSCs.

To the best of our knowledge, there has been no previous study exploring the roles of BMSCs infected with lentivirus carrying BMP9 (LV-BMP9) and co-cultured with P3HB4HB in the regeneration of bone defects. In this study, we infected BMSCs with LV-BMP9 and then cultured the cells on P3HB4HB scaffolds. This study aimed to investigate the effects and mechanism of a composite tissue engineered bone material consisting of bone mesenchymal stem cells, BMP9 gene lentiviral vector, and P3HB4HB thermogel (BMSCs-LV-BMP9-P3HB4HB) on calvarial skull defects in rats.

Material and Methods

Animals

Sprague-Dawley (SD) rats aged 2 weeks were obtained from the Experimental Animal Center of Guizhou Medical University and were housed at 23–25°C, 50% humidity, and a light/dark cycle of 12 h/12 h, with free access to food and water. The animal experiments were performed in accordance with the Declaration of Helsinki [18] and were approved by the Ethics Committee of the First Affiliated Hospital of Chongqing Medical University, Chongqing, China.

BMSCs isolation

The BMSCs were isolated from rats using a previously described protocol [19] with some modifications. Briefly, the SD rats were anesthetized by intraperitoneally injecting alpha chloralose (55 mg/kg). The bone marrow was isolated from tibias and fibulas of rats, washed with phosphate-buffered

saline (PBS), and cultured with Dulbecco's modified Eagle's medium F12 (DMEM-F12) medium (Gibco BRL. Co., Grand Island, NY, USA) containing 10% fetal bovine serum (FBS, Gibco BRL.) and 100 µg/ml streptomycin/100 U/ml penicillin (Beyotime Biotech, Shanghai, China). After culturing for 48 h, the medium was replaced, and the retained adherent cells were considered to be the BMSCs.

Induction of adipocyte and osteoblast differentiation

BMSCs were seeded onto 6-well plates (Corning-costar, Corning, NY, USA) containing adipogenic-differentiation DMEM (with insulin, FBS, dexamethasone, indomethacin, and IBMX) or osteogenic differentiation DMEM (with dexamethasone, β-glycerophosphate, and ascorbic acid) for 2 weeks, as instructed by the manufacturer (Sigma-Aldrich, St. Louis, MI, USA). After induction, the adipogenic potential and osteogenic potential of BMSCs were evaluated by oil-red O (ORO) staining (Cat. No. DL0009, Leagene Biotech Co., Beijing, China) and Alizarin red staining (Cat No. DZ0201, Leagene Biotech Co.), as described in a previous study [20]. Osteogenic differentiation of BMSCs was also evaluated by alkaline phosphatase (ALP) staining (Cat. No. DE0001, Leagene Biotech Co.) as described in a previous study [19].

Preparation and observation for BMSCs-P3HB4HB composite scaffold

After cultured BMSCs achieved 80% confluence, they were digested with 0.25% trypsin (Beyotime Biotech) and suspended in 10% FBS pre-treated (2 h) P3HB4HB scaffold at a density of 2×10^6 cell/ml. The BMSCs-P3HB4HB composite scaffold was cultured at 37°C and 5% CO_2 for 7-day passaging of cells, with fresh medium provided every 3 days. Subsequently, the morphology of the BMSCs-P3HB4HB composite scaffold was observed using a scanning electron microscope (SEM, Hitachi, Tokyo, Japan) at 1 day, 3 days, and 7 days after culture.

Determination for effects of P3HB4HB on proliferation and cell cycle of BMSCs

Cell-Counting Kit 8 (CCK-8) assay was used to determine cell viability of BMSCs combined with and without P3HB4HB scaffold, as described in a previous study [12]. After culturing for 1 day, 3 days, and 7 days, BMSCs were incubated with CCK-8 reagent (Cat. No. 96992, Sigma-Aldrich) for 2 h at 37°C and 5% CO_2. Absorbance density (OD) was measured with an enzyme-linked immunosorbent assay (ELISA) reader (Model: Multiskan FC, Thermo Scientific Pierce, Rockford, IL, USA) at 450 nm. For the cell cycle assay, BMSCs were harvested and permeabilized in ethanol (70%) at 4°C overnight, after which RNase was used to incubate cells for 30 min at 37°C. Subsequently, BMSCs were incubated using propidium iodide (PI) for another 30 min at 4°C.

Table 1. Specific primers for the RT-PCR assay amplifying RUNX-2, OCN, OPN, OSX, and BMP9.

Genes		Sequences (5'-3')
RUNX-2	Forward	TTCAAGGTTGTAGCCCTCGG
	Reverse	TGAAACTCTTGCCTCGTCCG
OCN	Forward	ATGGCACCACCGTTTAGG
	Reverse	GTGCCGTCCATACTTTCG
OPN	Forward	AAGGACCAACTACAACCA
	Reverse	CATCTGAGTGTTTCGTGT
OSX	Forward	ATGCCAATGACTACCCACCC
	Reverse	ATGGATGCCCGCCTTGTA
BMP9	Forward	GAGTGCCGTGAAGCGTTGG
	Reverse	GTCCCATTGCTGCGGTCA
GAPDH	Forward	GGCAAGTTCAACGGCACAG
	Reverse	CGCCAGTAGACTCCACGACAT

RUNX2 – runt-related transcription factor 2; OCN – osteocalcin; OPN – osteopontin; OSX – osterix; BMP9 – bone morphogenetic protein.

Finally, cell cycle distribution was evaluated with FACSVantage SE flow cytometry (BD Biosciences, San Jose, CA, USA).

LV-BMP9 infected BMSCs

After passaging for 3 generations, BMSCs were digested with 0.25% trypsin (Beyotime Biotech), re-suspended, seeded, and cultured for 3 h at 4°C and 5% CO_2. Subsequently, BMSCs were transfected with LV-BMP9 or blank LV vector at 50 multiplicity of infection (MOI) and cultured for 4 h, followed by refreshing the medium. The blank LV vector was employed as a negative control and LV-BMP9 was used as the experimental group. After culturing for 7 days, BMSCs were observed under a fluorescent microscope (Model: ECLIPSE Ti-S, Olympus, Tokyo, Japan) to assess the infection efficiency. The blank LV vector and LV-BMP9 were synthesized and provided by Western Biotech Co. (Chongqing, China).

Real-time PCR assay (RT-PCR)

The total RNAs in BMSCs were extracted with cell lysis solution (Beyotime Biotech). The complementary DNAs (cDNAs) were synthesized using a reverse transcription kit (Western Biotech, Chongqing, China) according to the manufacturer's instructions. mRNA expression of osteogenic factors, including runt-related transcription factor 2 (RUNX-2), osteocalcin (OCN), osteopontin (OPN), osterix (OSX), and BMP9, were measured using a SYBR Green I RT-PCR kit (Western Biotech). GAPDH was used as the internal control for qRT-PCR assay. The RT-PCR assay was conducted using the ABI StepOne Plus Real-Time PCR

system (ABI, Foster City, CA, USA). Primers for these osteogenic factors are listed in Table 1. Gene expressions of osteogenic factors were evaluated using $2^{-\Delta\Delta ct}$ method [21].

Western blot assay

The BMSCs were lysed using Cell Lysis Buffer for Western (Cat. No. P0013, Beyotime Biotech) to obtain proteins, according to the manufacturer's instructions. The concentrations of obtained proteins were determined using an Enhanced BCA Protein Assay Kit (Cat. No. P0010S, Beyotime Biotech). The same dosages of proteins were added to the sodium dodecyl sulphate-polyacrylamide gel electrophoresis (SDS-PAGE, Ameresco, Inc., Solon, OH, USA) and electric-transferred onto the polyvinylidene fluoride (PVDF) membranes (Bio-Rad Lab., Hercules, CA, USA). Then, PVDF membranes were treated with mouse anti-rat RUNX2 monoclonal antibody (Cat. No. 76956), mouse anti-rat OCN monoclonal antibody (Cat. No. ab13420), rabbit anti-rat OSX polyclonal antibody (Cat. No. ab22552), and rabbit anti-rat GAPDH (Cat. No. ab9485) overnight at 4°C, followed by incubation with horseradish peroxidase (HRP)-labeled rabbit anti-mouse IgG (Cat. No. ab9385) or HRP-labeled goat anti-rabbit IgG (Cat. No. ab6721) at 37°C for 2 h. All of the above primary and secondary antibodies were purchased from Abcam Biotech (Cambridge, MA, USA). The Western blots were stained with a Pierce ECL Western Blotting Substrate (Cat. No. 32106, Thermo Scientific Pierce, Rockford, IL, USA). The Western blot images were captured and analyzed using Labworks 4.6 Analysis software (Labworks, Upland, CA, USA).

Establishment of calvarial bone defect rat model

The calvarial bone defect rat model was established as described in previous studies [22,23] with a few modifications. Briefly, the rats were intraperitoneally anaesthetized with alpha chloralose (55 mg/kg). The area of the skin covering the calvaria were shaven and disinfected using 70% ethanol. The calvaria of rats were exposed by creating circular defects 5 mm in diameter, using a high-speed skull drill (Zhenghua Bio. Co., Anhui, China). The established calvarial bone defect rats were divided into a calvarial defect model group (without transplantation of any materials), a BMSC+LV+P3HB4HB group (transplanting the BMSC+LV-P3HB4HB composite material onto the skull wound), and a BMSC+LV-BMP9+P3HB4HB group (transplanting the BMSC+LV-BMP9-P3HB4HB composite material onto the skull wound). Rats in the sham group only had the scalp opened, without creation of a bone defect. After 4 weeks of transplantations, the injured skulls were removed and treated with 4% paraformaldehyde (Sangon Biotech. Co., Shanghai, China) for subsequent micro-CT analysis, Masson's trichrome staining, hematoxylin and eosin (H&E) staining, and immunohistochemistry (IHC).

Micro-computed tomography (micro-CT) measurement

The specimens (injured skulls) in different groups were fixed with 4% paraformaldehyde for 24 h and scanned with a micro-CT scanner (Model: Scanco Medical viva CT 40, provided by Chongqing Stomatological Hospital, Chongqing, China). The parameters were set as: X-ray voltage of 50 kV, working current of 145 mA, isotropic-voxel size of 12 μm, and aluminum filter of 1 mm. The imaging data, including bone volume of newly regenerated bone and bone regenerations, were analyzed with CT-An software (Bruker, Kontich, Belgium) after standardized reconstructing.

Histological evaluation for bone regeneration

The regenerations of newly-formed bones were assessed by H&E staining and Masson's trichrome staining. Following micro-CT analysis, the specimens (injured skulls) were fixed with 4% paraformaldehyde and paraffin embedded. The histological sections (5-μm) were cut and prepared from the injured skull tissues using a freezing microtome (Model: RM 2145, Leica, Frankfurt, Germany). The sections were then incubated with xylene (SinoPharm Med. Co., Shanghai, China) for 15 min and washed with 100% ethanol for 10 min, 90% ethanol for 10 min, and 75% ethanol for 10 min, followed by gradient-ethanol dewaxing to water. Then, the sections were stained with hematoxylin (Jiancheng Bioengineering Institute, Nanjing, China) and eosin (Beyotime Biotech) to assess pathological changes in newly-formed bones. Moreover, sections were also stained with Masson (Leagene Biotech. Co., Beijing, China) to assess changes in collagen fibers in newly-formed bones, according to the manufacturer's instructions. Images of H&E staining and Masson's trichrome staining were captured through an optical microscope (Model: IX71, Olympus, Tokyo, Japan).

Immunohistochemistry assay

The formed bones were fixed with 4% paraformaldehyde, embedded in paraffin, cut into sections (5-μm), and treated with 3% hydrogen peroxide (Beyotime Biotech) for 15 min to inactivate endogenous-peroxidase activity. The sections were blocked with 1% bovine serum albumin (BSA) at room temperature for 60 min and then incubated using rabbit anti-rat OSX polyclonal antibody (Cat. No. ab22552), mouse anti-rat OCN monoclonal antibody (Cat. No. ab13420), rabbit anti-rat OSX polyclonal antibody (Cat. No. ab22552), and mouse anti-rat RUNX2 monoclonal antibody (Cat. No. 76956) at 4°C overnight. Subsequently, sections were washed with PBS 3 times and incubated with HRP-conjugated rabbit anti-mouse IgG (Cat. No. ab9385) or HRP-labeled goat anti-rabbit IgG (Cat. No. ab6721) at room temperature for 1 h. The stained sections were subjected to diaminobenzidine (DAB, 5 min), hematoxylin (5 min), alcohol dehydration (75%, 85%, 95%, and 100% for 3 min, respectively), xylene, and sealed with neutral gum. The stained sections were observed using a
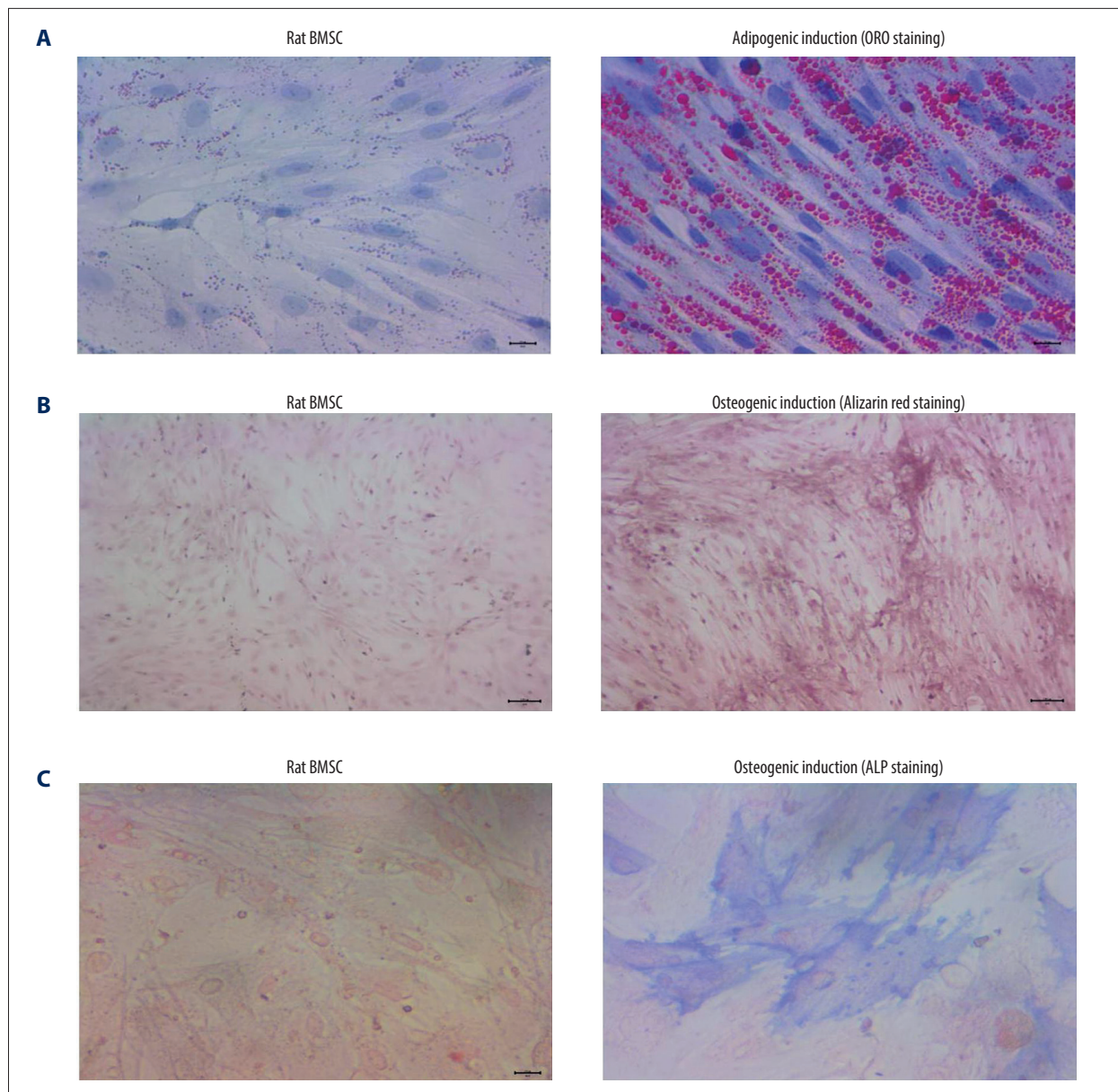
Figure 1. BMSCs derived from rats demonstrated obvious adipogenic potential and osteogenic potential. (**A**) Adipogenic differentiation of BMSCs determined by ORO staining. (**B**) Osteogenic differentiation of BMSCs determined by Alizarin red staining. (**C**) Osteogenic differentiation of BMSCs by ALP staining. ORO – oil-red O staining; BMSCs – bone mesenchymal stem cells; ALP – alkaline phosphatase.

microscope (Model: IX71, Olympus, Tokyo, Japan) and photographed at a magnification of 100×.

Statistical analysis

Data are presented as mean±standard deviation (SD) and were analyzed with SPSS software 20.0 (SPSS Inc., Chicago, IL, USA). Tukey's post hoc test-validated ANOVA was used to analyze the differences among groups. $p<0.05$ was regarded as a statistically significant difference.

Results

BMSCs showed adipogenic and osteogenic differentiation potential

Adipogenic differentiation was evaluated using ORO staining, and the results indicated that BMSCs demonstrated no lipid droplets in the BMSCs group but demonstrated red-stained lipid droplets in the adipogenic induction group (Figure 1A). Alizarin red staining also showed that BMSCs demonstrated
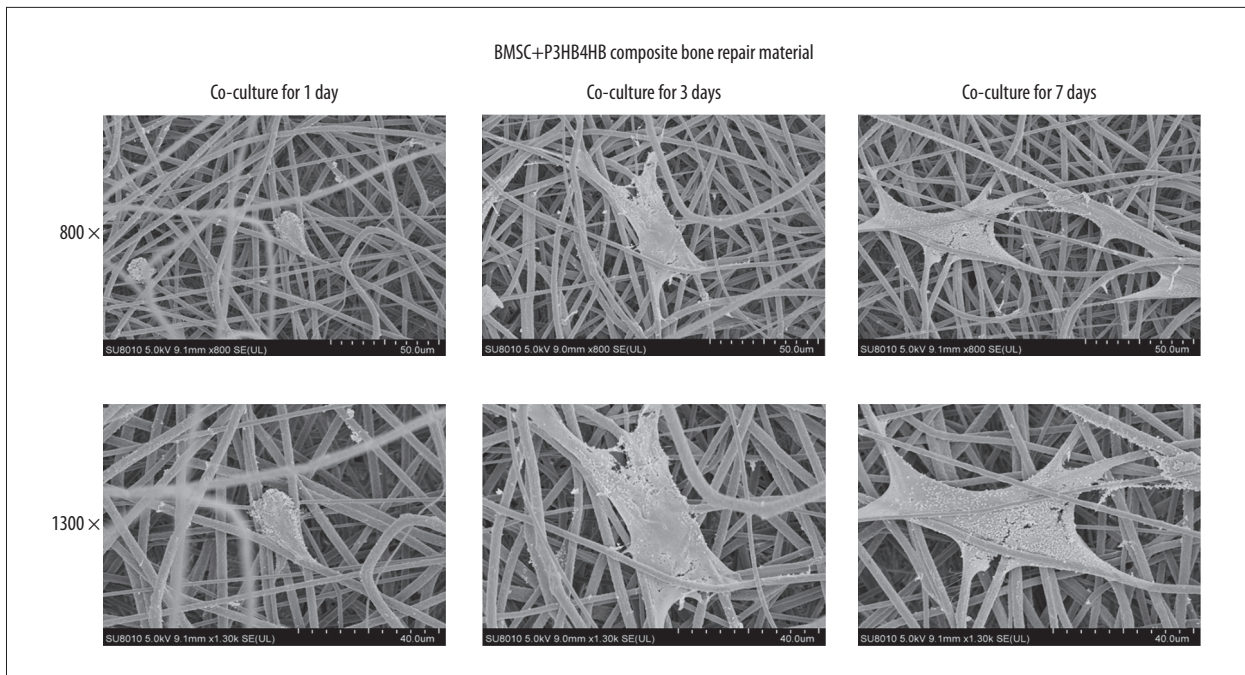
Figure 2. P3HB4HB scaffold demonstrated good biocompatibility with BMSCs from 1 day to 7 days after co-culture. BMSCs – bone mesenchymal stem cells.
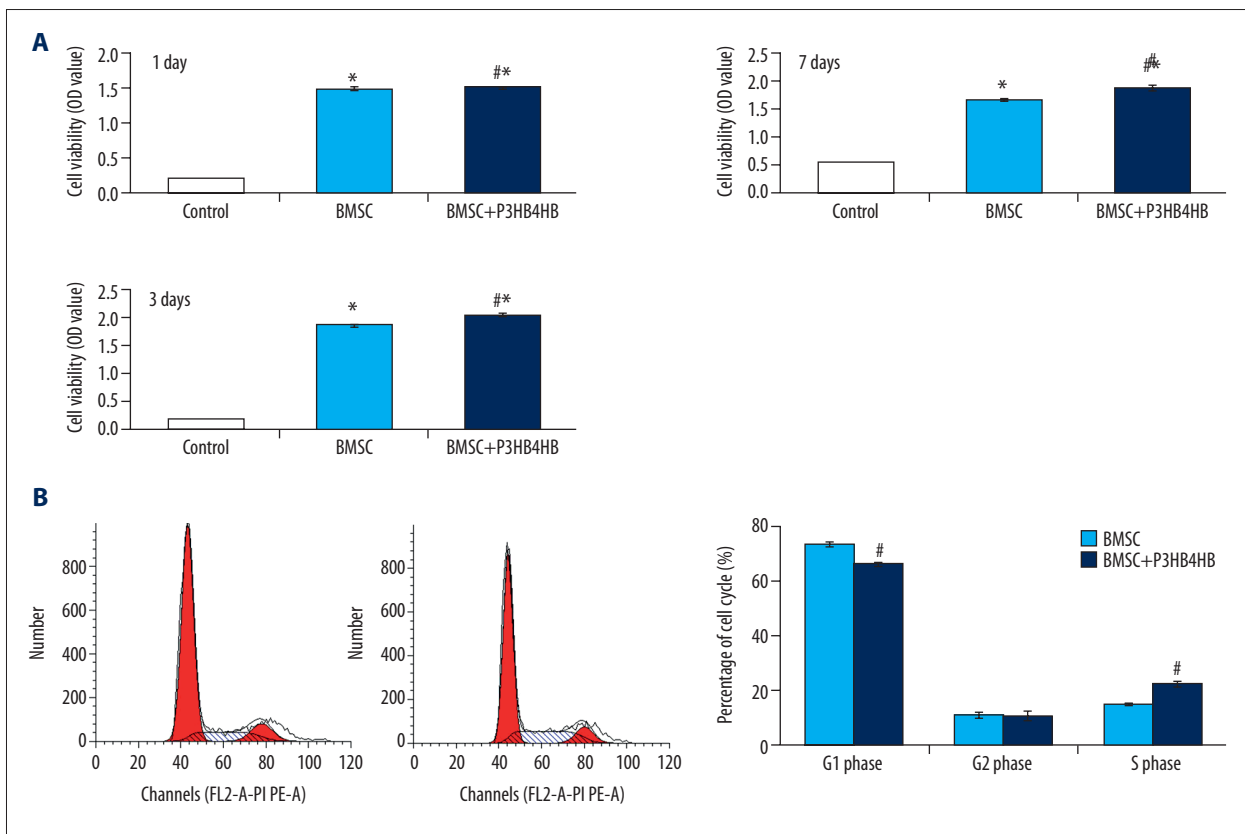

Figure 3. P3HB4HB scaffold co-culture increased the cell viability and modulated the cell cycle of BMSCs. (**A**) P3HB4HB scaffold promoted cell viability of BMSCs from 1 day to 7 days after co-culture. (**B**) P3HB4HB scaffold modulated cell cycle of BMSCs from 1 day to 7 days after co-culture. BMSCs – bone mesenchymal stem cells.
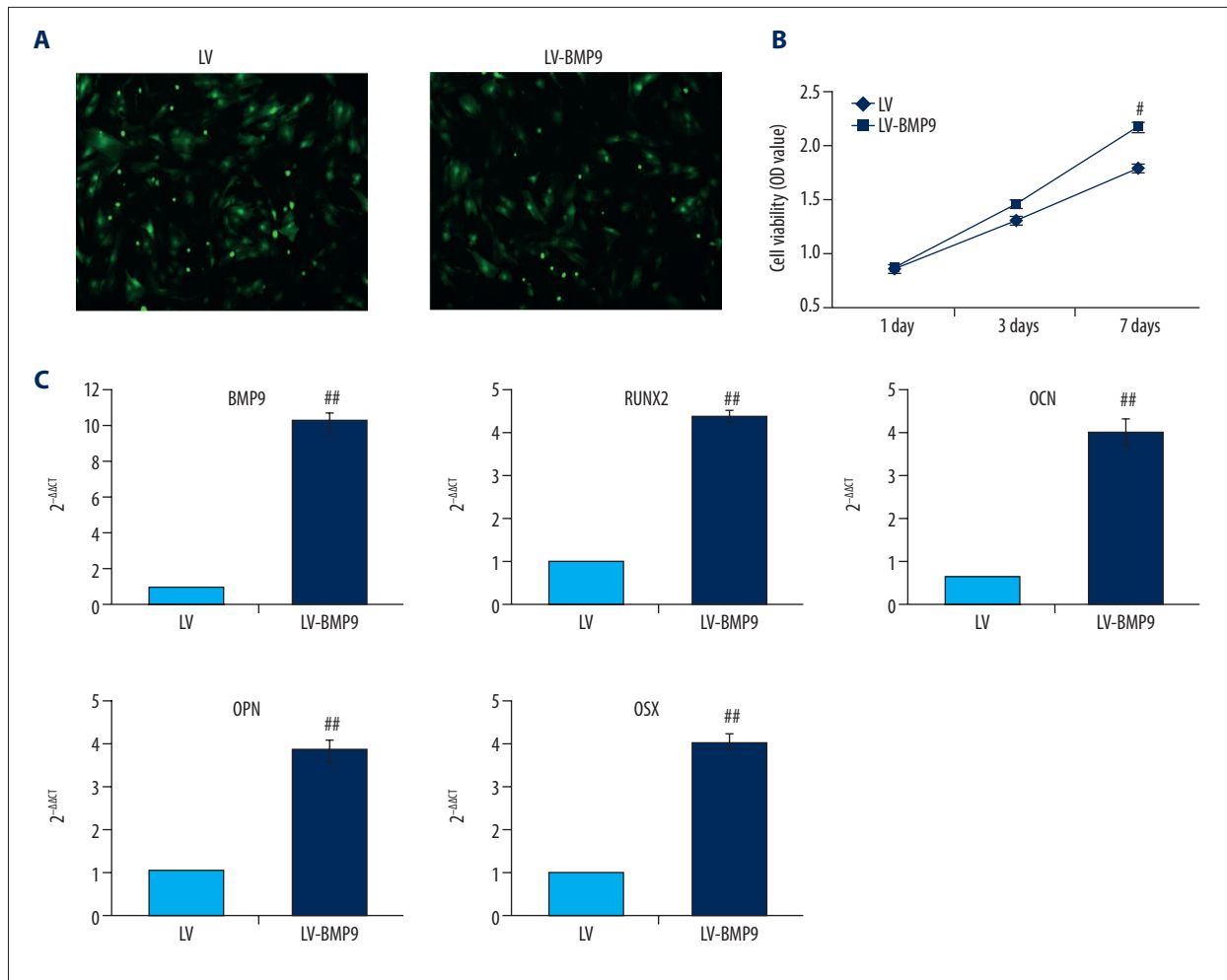
Figure 4. The LV-BMP9 infection enhanced cell viability and upregulated mRNA transcriptions of osteogenic factors (BMP9, RUNX2, OCN, OPN, OSX) in BMSCs. (**A**) Determination of LV or LV-BMP9 infection efficacy in BMSCs by immunofluorescence assay. (**B**) LV-BMP9 infection increased cell viability of BMSCs. (**C**) Expression of osteogenic factors, including BMP9, RUNX2, OCN, OPN, and OSX, was increased in LV-BMP9-infected BMSCs. # $p<0.05$ and ## $p<0.01$ versus the values of LV group. BMSCs – bone mesenchymal stem cells; RUNX2 – runt-related transcription factor 2; OCN – osteocalcin; OPN – osteopontin; OSX – osterix; BMP9 – bone morphogenetic protein.

remarkable reddish-brown mineralized nodules in the osteogenic induction group but there were no stained nodules in the BMSCs group (Figure 1B). Our results also indicated that there were obvious blue-stained cells in the osteogenic induction group but not in the BMSCs group (Figure 1C), which suggests that osteogenic induction triggers higher ALP activity.

BMSCs-P3HB4HB scaffold demonstrated cell-tissue compatibility

After 1 day, 3 days, and 7 days of co-culturing of BMSCs and P3HB4HB together, cell-tissue compatibility was observed using SEM. The results indicated that with the prolonged co-culturing time of BMSCs and P3HB4HB materials, the cell-tissue compatibility was remarkably increased (Figure 2).

BMSCs-P3HB4HB scaffold enhanced cell viability of BMSCs and modulated cell cycle

The CCK-8 results indicated that both BMSCs and BMSCs+P3HB4HB significantly enhanced cell viability compared to that of the control group at 1 day, 3 days, and 7 days of co-culturing (Figure 3A, $p<0.05$). BMSCs+P3HB4HB also demonstrated significantly higher cell viability compared to that in the control group after 3 days and 7 days of co-culturing (Figure 3A, $p<0.05$). Furthermore, the G1 phase percentage was significantly decreased and S phase was significantly increased in the BMSCs+P3HB4HB group compared to that in the BMSCs group (Figure 3B, $p<0.05$).
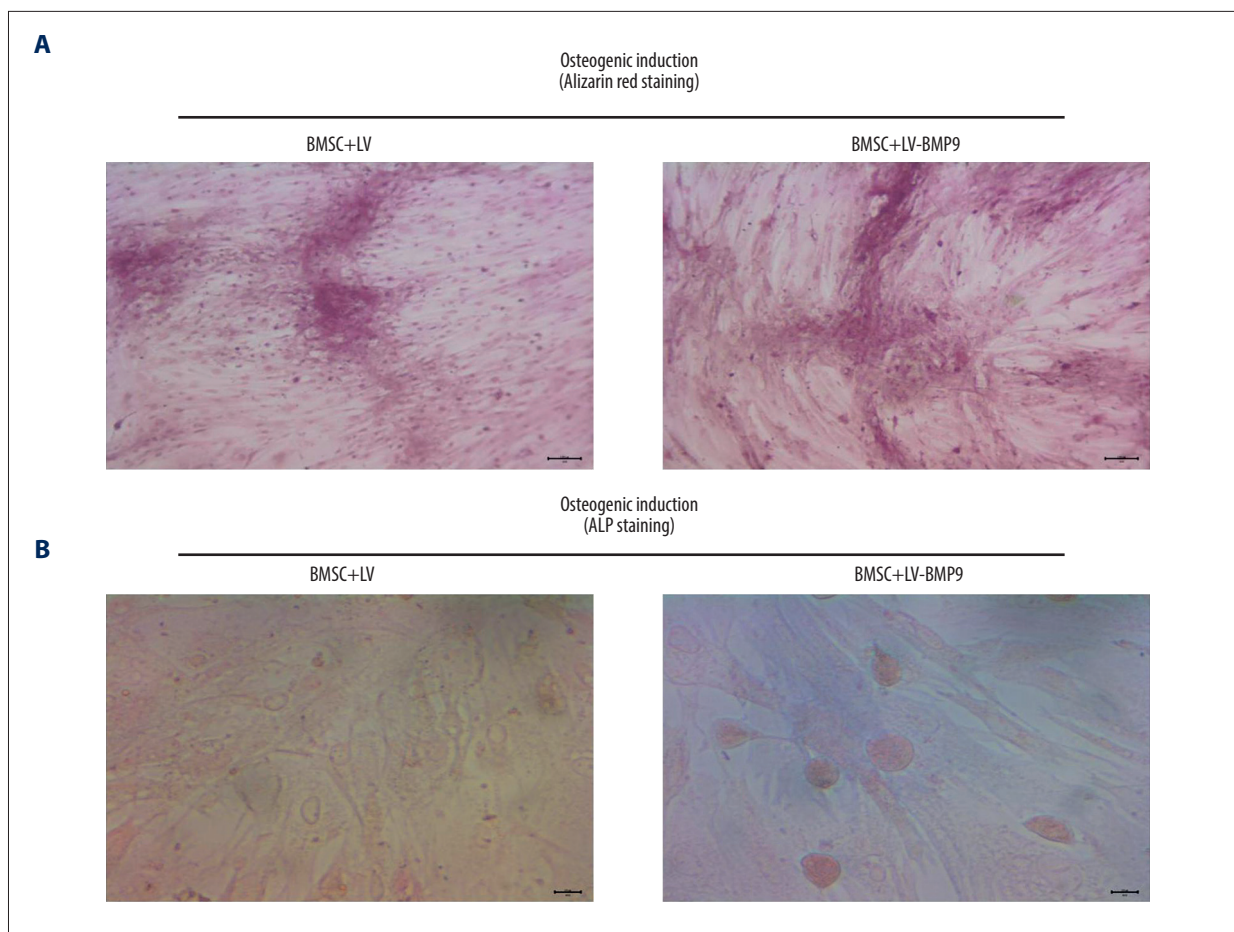
Figure 5. LV-BMP9 infection further triggered the osteogenic differentiation of the BMSCs according to both Alizarin red staining and ALP staining. (**A**) LV-BMP9 infection promoted osteogenic differentiation of BMSCs due to Alizarin red staining. (**B**) LV-BMP9 infection promoted osteogenic differentiation of BMSCs according to ALP staining. BMSCs – bone mesenchymal stem cells; BMP9 – bone morphogenetic protein; ALP – alkaline phosphatase.

BMP9-triggered osteogenic differentiation of BMSCs

To evaluate osteogenic effects of BMP9, the LV-BMP8 viral vector was synthesized and infected to BMSCs. The LV-BMP9 infection illustrated higher expressing efficacy (Figure 4A) and significantly increased cell viability of BMSCs compared to that in the LV infection group after 7 days of culturing (Figure 4B, $p<0.05$). LV-BMP9 infection significantly increased mRNA expression of osteogenic factors, including RUNX2, OCN, OPN, and OSX, compared to that in LV-infected BMSCs (Figure 4C, $p<0.01$).

Moreover, both Alizarin red staining (Figure 5A) and ALP staining (Figure 5B) findings also indicated BMSC+LV-BMP9 demonstrated significantly higher levels of osteogenic induction from BMSCs compared to that in the BMSC+LV group.

BMSCs-LV-BMP9-P3HB4HB triggered osteogenic differentiation

The Alizarin red staining (Figure 6A) and ALP staining (Figure 6B) results showed that with the prolonged culturing time (ranging from 7 days to 21 days), the osteogenic induction in BMSCs-LV-BMP9-P3HB4HB composite bone repair material was remarkably higher compared to that in BMSCs-LV -P3HB4HB material.

BMSCs-LV-BMP9-P3HB4HB promoted osteogenic factors expression

In this study, the osteogenic factors, including RUNX2, OCN, OPN, and OSX, were examined using Western blot assay (Figure 7A). The results indicated that RUNX2 expression (Figure 7B), OCN expression (Figure 7C), OPN expression (Figure 7D), and OSX expression (Figure 7E) in the BMSCs-LV-BMP9-P3HB4HB group were significantly higher compared to
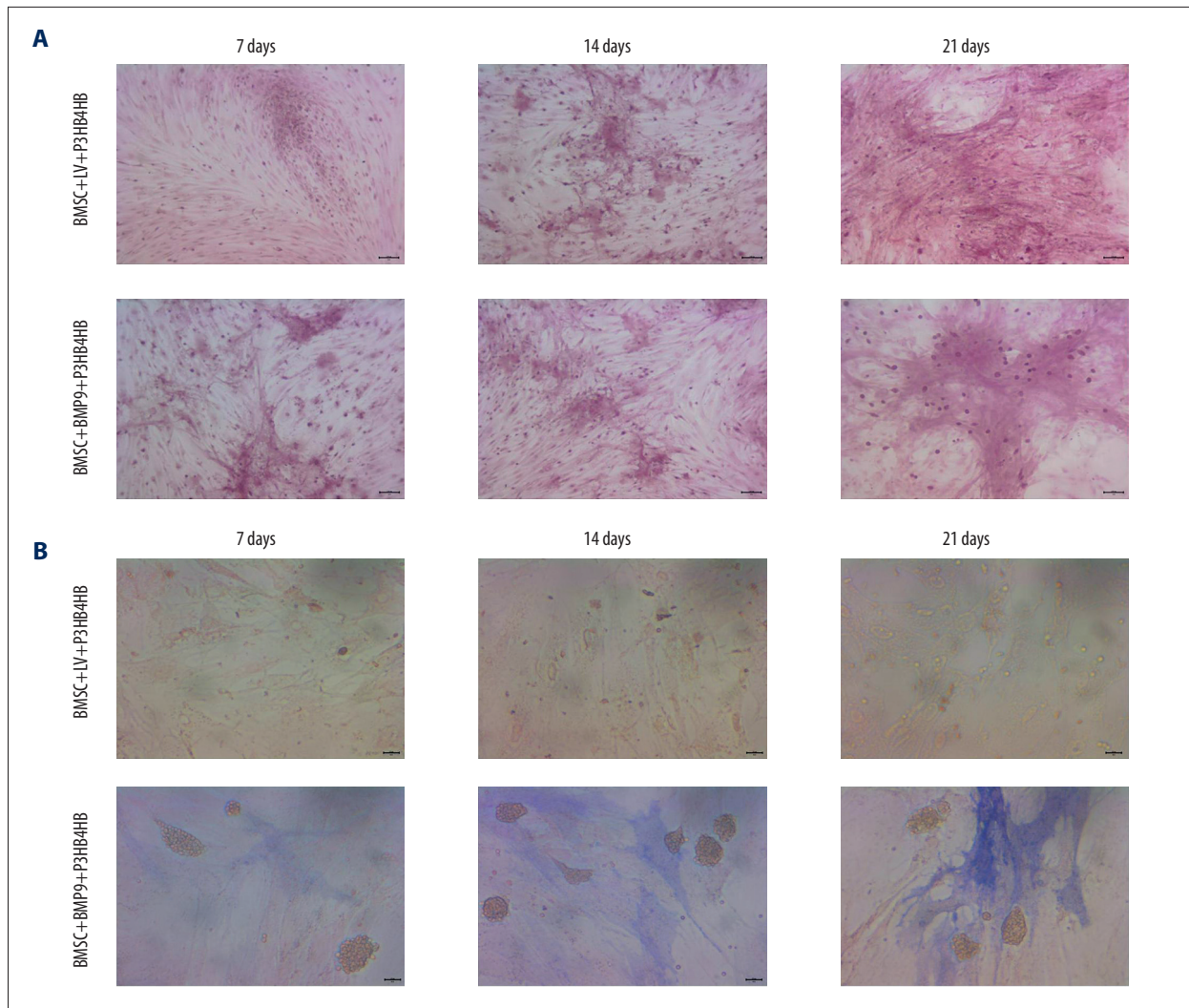
Figure 6. BMSCs-LV-BMP9-P3HB4HB significantly triggered osteogenic differentiation of BMSCs at 1 day, 3 days, and 7 days after co-culture, according to both Alizarin red staining and ALP staining. (**A**) Alizarin red staining for osteogenic differentiation of BMSCs. (**B**) ALP staining for osteogenic differentiation of BMSCs. BMSCs – bone mesenchymal stem cells; BMP9 – bone morphogenetic protein; ALP – alkaline phosphatase.

that in the BMSCs-LV-P3HB4HB group (*p*<0.05) after 7 days, 14 days, and 21 days of BMSCs culturing.

BMSCs-LV-BMP9-P3HB4HB demonstrated stronger repair ability

The micro-CT findings showed that there were no skull defects in rats in the sham group but there were obvious defects in the calvarial defect model rats (Figure 8). Importantly, compared with calvarial defect model rats, the BMSCs-LV-P3HB4HB composite scaffold demonstrated some obvious repair ability, but BMSCs-LV-BMP9-P3HB4HB composite bone repair material had stronger repair ability (Figure 8).

BMSCs-LV-BMP9-P3HB4HB alleviated pathological injury and increased collagen fiber production

The H&E staining results showed that BMSCs-LV-BMP9-P3HB4HB composite bone repair material significantly alleviated the pathological injury of calvarial defect model rats (Figure 9A). Furthermore, compared with calvarial defect model rats, there were more collagen fibers in the BMSCs-LV-P3HB4HB composite scaffold group, and increased more in the BMSCs-LV-BMP9-P3HB4HB composite bone repair material group (Figure 9B).
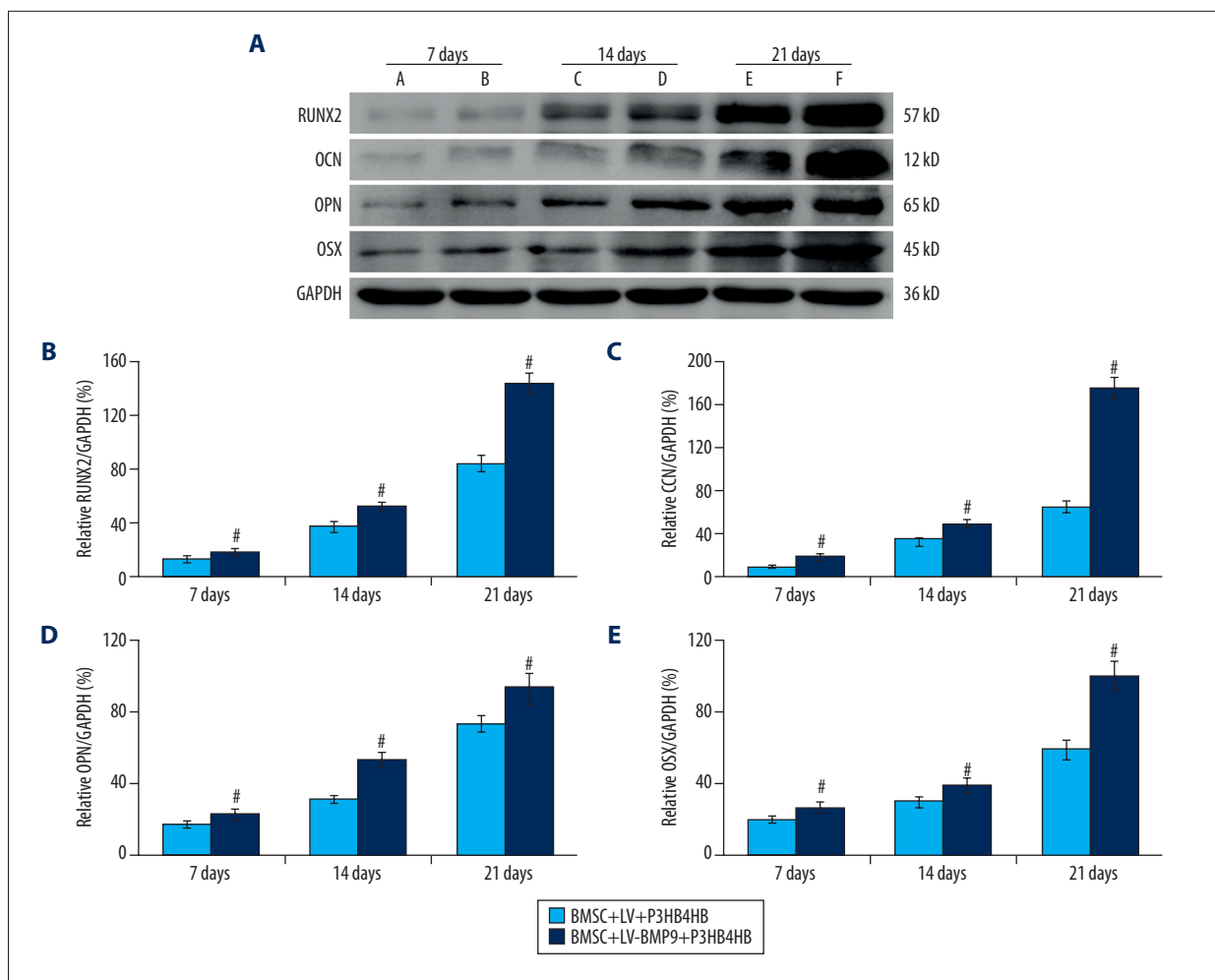
Figure 7. BMSCs-LV-BMP9-P3HB4HB composite bone repair material increased the expression of osteogenic factors, including BMP9, RUNX2, OCN, OPN, and OSX. (**A**) Expression of osteogenic factors evaluated by Western blot assay. (**B**) Effects of MSCs-LV-BMP9-P3HB4HB on RUNX2 expression. (**C**) Effects of MSCs-LV-BMP9-P3HB4HB on OCN expression. (**D**) Effects of MSCs-LV-BMP9-P3HB4HB on OPN expression. (**E**) Effects of MSCs-LV-BMP9-P3HB4HB on OSX expression. # $p<0.05$ versus the values of BMSC+LV-P3HB4HB group. BMSCs – bone mesenchymal stem cells; RUNX2 – runt-related transcription factor 2; OCN – osteocalcin; OPN – osteopontin; OSX – osterix; BMP9 – bone morphogenetic protein.

BMSCs-LV-BMP9-P3HB4HB triggered osteogenic factors expression in calvarial defect model rats

The immunohistochemistry assay results showed that BMSCs-LV-BMP9-P3HB4HB composite bone repair material transplantation remarkably triggered osteogenic factors expression, including RUNX2 (Figure 10A), OCN (Figure 10B), and OSX (Figure 10C), in calvarial defect model rats. These results suggest that BMSCs-LV-BMP9-P3HB4HB composite bone repair material repaired the injured skull tissues by triggering the expression of osteogenic factors.

Discussion

There are many clinical challenges in bone defect regeneration due to the loss of bone functions and difficulty of bone repair [24]; therefore, it is critical to develop an effective bone repair material using a tissue engineering strategy. An appropriate tissue engineering repair material should be composed of 3 main elements: seeded cells, scaffold, and growth factors [25]. In the present investigation, we proved that BMSCs could grow effectively on a P3HB4HB scaffold and BMP9 could efficiently promote the adipogenic and osteogenic differentiation of BMSCs. Therefore, BMP9 expressing BMSCs co-cultured with P3HB4HB formed BMSCs-LV-BMP9-P3HB4HB composite bone repair material and demonstrated higher osteogenic effects on injury in a calvarial defect rat model.
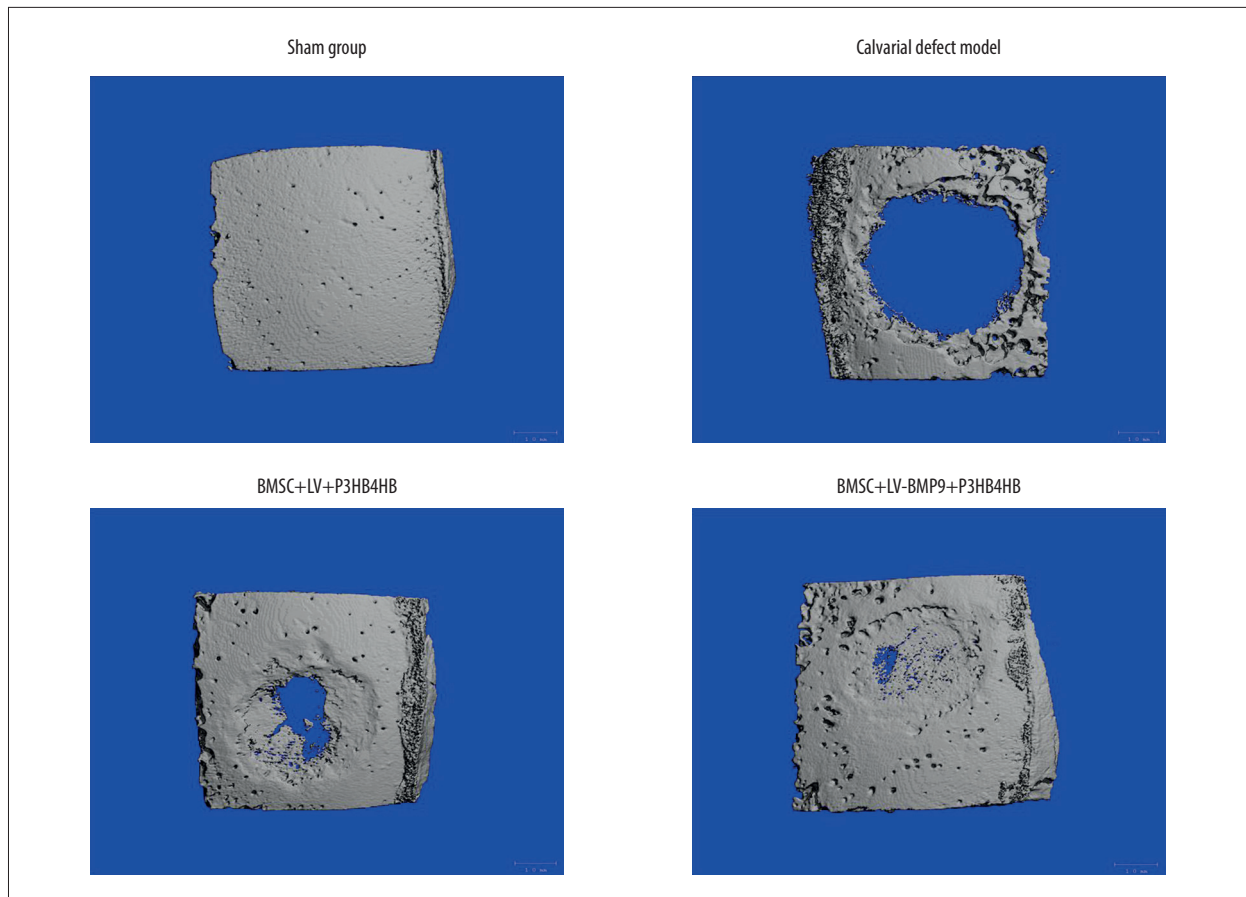
Figure 8. BMSC+LV-BMP9+P3HB4HB composite bone repair material demonstrated good repair ability for defect tissues of calvarial defect rats. The skull tissues in rat of sham group, calvarial defect model group, BMSC+LV+P3HB4HB group, and BMSC+LV-BMP9+P3HB4HB group are illustrated. BMSCs – bone mesenchymal stem cells.

BMSC are multi-differentiated cells that demonstrate the ability of differentiating into osteoblasts, with promising potential for repairing tissue defects [26]. When the BMSCs were seeded onto the P3HB43HB scaffold, they exhibited higher cell viability and stronger osteogenic differentiation ability. We found that the LV-BMP9-infected BMSCs demonstrated higher osteogenic capability and ALP activity. RT-PCR assay also showed that LV-BMP9 infection remarkably induced the mRNA expression of osteogenic factors, such as RUNX2, OCN, OPN, and OSX. All of these findings suggest that BMP-9 infection can remarkably promote the osteogenic differentiation ability of BMSCs, which is consistent with a previous study [17].

P3HB4HB is considered to be a composite scaffold with good biocompatibility, and is suitable for use in tissue engineering [12,27]. In the present study, the transmission electron microscopy (TEM) images demonstrated that BMSCs adhered closely to and proliferated on the P3HB4HB scaffold due to its core-shell structure and mechanical characteristics [28]. Our results indicate that when cultured on the P3HB4HB scaffold, BMSCs have higher cell viability, which suggests that P3HB4HB

facilitates the proliferation of BMSCs. Therefore, P3HB4HB shows promise as a scaffold for BMSCs co-culture and an implant for injured tissues.

In this study, we attempted to determine whether the LV-BMP9-infected BMSCs integrating P3HB4HB benefit the regeneration of defected skull bones. As previous studies described [29,30], the BMP9 molecule, a member of the BMP protein family, is the most effective inducer for triggering osteogenesis of BMSCs. Recent studies [31,32] also demonstrated that BMP9 administration remarkably promotes the regeneration and repair of injured bones. Therefore, we structured BMSCs-LV-BMP9-P3HB4HB composite bone repair material using a tissue engineering approach for use in repair in a calvarial defect rat model. The micro-CT results showed that there were more novel regenerated bones in the BMSCs-LV-BMP9-P3HB4HB composite bone repair material-transplanted calvarial defect rats. The histological findings also indicated that MSCs-LV-BMP9-P3HB4HB composite bone repair material remarkably increased the osteogenic differentiation of MBSCs and promoted ALP activity *in vivo* and *in vitro*. All of the above
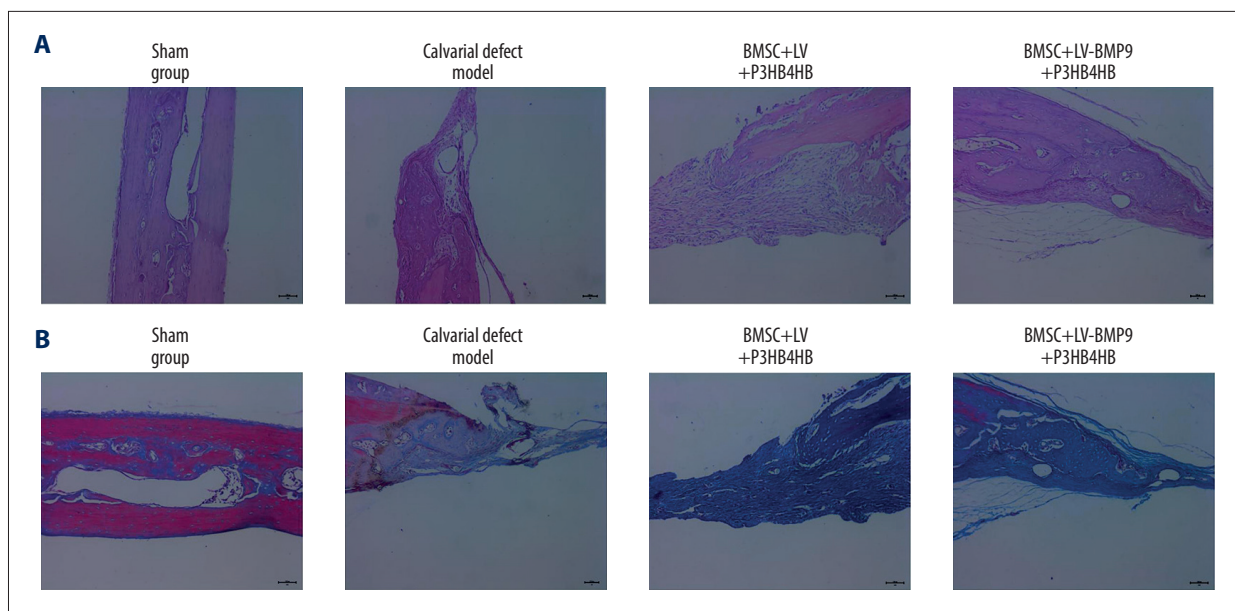
Figure 9. Changes of pathological injury and collagen fiber production in newly-formed tissues of calvarial defect rats. (**A**) Evaluation of pathological changes by H&E staining. (**B**) Determination of contents of collagen fibers by Masson's trichrome staining.
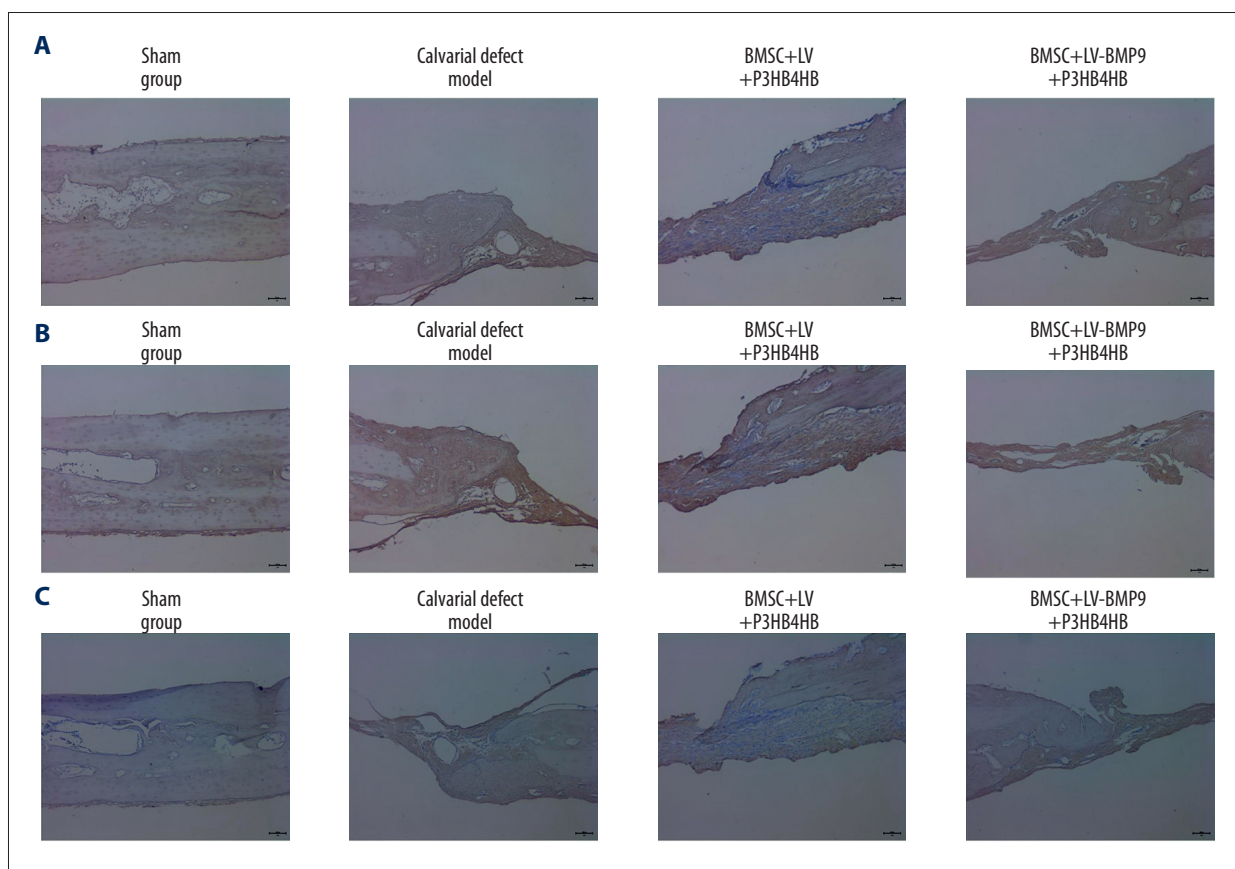

Figure 10. BMSC+LV-BMP9+P3HB4HB composite bone repair material promoted expression of osteogenic factors in novel regenerated tissues of calvarial defect rats, according to immunohistochemistry assay (IHC). (**A**) RUNX2 expression in regenerated tissues. (**B**) OCN expression in regenerated tissues. (**C**) OPN expression in regenerated tissues. BMSCs – bone mesenchymal stem cells; OCN – osteocalcin; OPN – osteopontin.

results demonstrate that BMP9 induction mediated the ALP and osteogenic activity of the BMSCs and promoted the regeneration of osteoblasts, after which the bone regeneration was initiated.

In this study, the tissue engineering-guided strategy combining BMP9 gene, BMSCs, and P3HB4HB scaffold demonstrated the best repairing effects on calvarial defect of rats. However, there are some limitations in the present study. First, the generated bone repair material had some of the same limitations as reported with previously constructed materials or scaffolds [13,17,33,34], such as problems with long-term effectiveness, security of materials, and stability of materials. In future research we will attempt to overcome these limitations of the material. Second, we used rats, not mice, to generate the calvarial defect model because the larger size of rats makes surgery easier. However, the transgenic mouse model could better identify calvarial tissue origins, signaling pathways involved in during healing, and possible strategies to enhance bone formation [35]. In subsequent research using a calvarial defect model, we plan to use the mouse model and to explore the signaling pathways and biomarkers participating in calvarial tissue repair in transgenic mice.

Conclusions

The present study created an implant combining LV-BMP9-infected BMSCs and P3HB4HB scaffold, named as BMSCs-LV-BMP9-P3HB4HB composite bone repair material. BMP9-expressing BMSCs demonstrated higher osteogenic differentiation when co-cultured on the P3HB4HB scaffold. BMSCs-LV-BMP9-P3HB4HB composite bone repair material effectively repaired the injured skull tissues of the calvarial defect rats. This bone repair material may have applications in tissue engineering for regeneration of bone defects.

Conflict of interest

None.

References:

1. Holzwarth JM, Ma PX: Biomimetic nanofibrous scaffolds for bone tissue engineering. Biomaterials, 2011; 32: 9622–29

2. Zhang R, Liu J, Yu S et al: Osteoprotegerin (OPG) promotes recruitment of endothelial progenitor cells (EPCs) via CXCR4 signaling pathway to improve bone defect repair. Med Sci Monit, 2019; 25: 5572–79

3. Kolambkar YM, Boerckel JD, Dupont KM et al: Spatiotemporal delivery of bone morphogenetic protein enhances functional repair of segmental bone defects. Bone, 2011; 49: 485–92

4. Frohbergh ME, Katsman A, Botta GP et al: Elecrospun hydroxyapatite-containing chitosan nanofibers crosslinked with genipin for bone tissue engineering. Biomaterials, 2012; 33: 9167–78

5. Kolambkar YM, Dupont KM, Boerckel JD et al: An alginate-based hybrid system for growth factor delivery in the functional repair of large bone defects. Biomaterials, 2011; 32: 65–74

6. Naros A, Bayazeed B, Schwarz U et al: A prospective histomorphometric and cephalometric comparison of bovine bone substitute and autogenous bone grafting in Le Fort I osteotomies. J Craniomaxillofac Surg, 2019; 47: 233–38

7. Dang M, Saunders L, Niu X et al: Biomimetic delivery of signals for bone tissue engineering. Bone Res, 2018; 6: 25

8. Bhattacharjee P, Kundu B, Naskar D et al: Silk scaffolds in bone tissue engineering: An overview. Acta Biomater, 2017; 63: 1–17

9. Chen C, Zhu C, Hu X et al: Alpha-hemihydrate calcium sulfate/octacalcium phosphate combined with sodium hyaluronate promotes the marrow-derived mesenchymal stem cell osteogenesis in vitro and in vivo. Drug Des Devel Ther, 2018; 12: 3269–87

10. Porter JR, Ruckh TT, Popat KC: Bone tissue engineering: A review in bone biomimetics and drug delivery strategies. Biotechnol Prog, 2009; 25: 1539–60

11. Chang HC, Sun T, Sultana N et al: Conductive PEDOT: PSS coated polylactide (PLA) and ploy (3-hydroxybutyrate-co-3-hydroxyvalerate) (PHBV) electrospun membranes: Fabrication and characterization. Mater Sci Eng C Mater Biol Appl, 2016; 61: 396–410

12. Ma MX, Liu Q, Ye C et al: Preparation of P3HB4HB/(Gelatin+PVA) composite scaffolds by coaxial electrospinning and its biocompatibility evaluation. Biomed Res Int, 2017; 2017: 9251806

13. Liu Z, Chang H, Hou Y et al: Lentivirus-mediated microRNA-26a overexpression in bone mesenchymal stem cells facilitates bone regeneration in bone defects of calvaria in mice. Mol Med Rep, 2018; 18: 5317–26

14. Futrega K, Atkinson K, Lott WB et al: Spheroid coculture of hematopoietic stem/progenitor cells and monolayer expanded mesenchymal stem/stromal cells in polydimethylsiloxane microwells modestly improves in vitro hematopoietic stem/progenitor cell expression. Tissue Eng Part C Methods, 2017; 23: 200–18

15. Carlisle E, Fischgrund JS: Bone morphogenetic proteins for spinal fusion. Spine J, 2005; 5: 240S–49S

16. Li J, Ma J, Zhang X et al: Long non-coding RNA (lncRNA)/OP-responsive gene (BORG) promotes development of chemoresistance of colorectal cancer cells to carboplatin. Med Sci Monit, 2020; 26: e919103

17. Nie L, Yang X, Duan L et al: The healing of alveolar bone defects with novel bio-implants composed of Ad-BMP-9-transfected rDFCs and CHA scaffolds. Sci Rep, 2017; 7: 6373

18. Williams JR: The declaration of Helsinki and public health. Bull World Health Organ, 2008; 86: 650–52

19. Gu C, Xu Y, Zhang S et al: miR-27a attenuates adipogenesis and promotes osteogenesis in steroid-induced rat BMSCs by targeting PPAR-gamma and GREM1. Sci Rep, 2016; 6: 38491

20. Fang S, Li Y, Chen P: Osteogenic effect of bone marrow mesenchymal stem cell-derived exosomes on steroid-induced osteonecrosis of the femoral head. Drug Des Devel Ther, 2018; 13: 45–55

21. Livak KJ, Schmittgen TD: Analysis of relative gene expression data using real-time quantitative PCR and the $2^{-\Delta\Delta ct}$ method. Methods, 2001; 25: 402–8

22. Kim JM, Kim JH, Lee BH et al: Vertical bone augmentation using three-dimensionally printed cap in the calvarial partial defect. In Vivo, 2018; 32: 1111–17

23. Gao R, Watson M, Callon KE et al: Local application of lactoferrin promotes bone regeneration in a rat critical-sized calvarial defect model as demonstrated by micro-CT and histological analysis. J Tissue Eng Regen Med, 2018; 12: e620–26

24. Giannoudis PV, Faour O, Goff T et al: Masquelet technique for the treatment of bone defects: Tips-tricks and future directions. Injury, 2011; 42: 591–98

25. Zheng P, Hu X, Lou Y et al: A rabbit model of osteochondral regeneration using three-dimensional printed polycaprolactone-hydroxyapatite scaffolds coated with umbilical cord blood mesenchymal stem cells and chondrocytes. Med Sci Monit, 2019; 25: 7361–69

26. Shi Y, Hu Y, Lv C et al: Effects of reactive oxygen species on differentiation of bone marrow mesenchymal stem cells. Ann Transplant, 2016; 21: 695–700

27. Raposo RS, de Almeida MCMD, da Fonseca MMR et al: Feeding strategies for tuning poly (3-hydroxybutyrate-co-4-hydroxybutyrate) monometic composition and productivity using *Burkholderia sacchari*. Int J Biol Macromol, 2017; 105: 8

28. Luo L, Wei X, Chen GQ: Physical properties and biocompatibility of poly (3-hydroxybutyrate-co-3-hydroxyhexanoate) blended with poly (3-hydroxybutyr-ate-co-4-dydroxybutyrate). J Biomater Sci Polym Ed, 2009; 20: 1537–53

29. Fujioka-Kobayashi M, Sawada K, Kobayashi E et al: Osteogenic potential of rhBMP9 combined with a bovine-derived natural bone mineral scaffold compared to rhBMP2. Clin Oral Implants Res, 2017; 28: 381–87

30. Zheng W, Gu X, Sun X et al: FAK mediates BMP9-induced osteogenic differentiation via Wnt and MAPK signaling pathway in synovial mesenchymal stem cells. Artif Cells Nanomed Biotechnol, 2019; 47: 2641–49

31. Xiang L, Liang C, Zhen-Yong K et al: BMP9-induced osteogenic differentiation and bone formation of muscle-derived stem cells. J Biomed Biotechnol, 2012; 2012: 610952

32. Yu L, Dawson LA, Yan M et al: BMP9 stimulates joint regeneration at digit amputation wounds in mice. Nat Commun, 2019; 10(1): 424

33. Song JL, Zheng W, Chen W et al: Lentivirus-mediated microRNA-124 gene-modified bone marrow mesenchymal stem cell transplantation promotes the repair of spinal cord injury in rats. Exp Mol Med, 2017; 49: e332

34. Ghate NS, Cui H: Mineralized collagen artificial bone repair material products used for fusing the podarthral joints with internal fixation, a case report. Regen Biomater, 2017; 4: 295–98

35. Murphy MP, Quarto N, Longaker MT et al: Calvarial defects: Cell-based reconstructive strategies in the murine model. Tissue Eng Part C Methods, 2017; 23: 971–81